NIH Public Access
Author Manuscript
J Neurol Sci. Author manuscript; available in PMC 2013 June 15.

Published in final edited form as:
J Neurol Sci. 2012 June 15; 317(1-2): 66–73. doi:10.1016/j.jns.2012.02.027.

Tunicamycin produces TDP-43 cytoplasmic inclusions in cultured brain organotypic slices

Cadman Leggett[1,2], **Daniel S. McGehee**[2], **James Mastrianni**[1], **Wenbin Yang**[1], **Tao Bai**[1], and **James R. Brorson**[1]

[1]Department of Neurology, The University of Chicago

[2]Department of Anesthesia and Critical Care, The University of Chicago

Abstract

The cellular distribution of TAR DNA binding protein (TDP-43) is disrupted in several neurodegenerative disorders, including frontotemporal lobar degeneration with ubiquitin-positive inclusions (FTLD-U subtype) and amyotrophic lateral sclerosis (ALS). In these conditions, TDP-43 is found in neuronal cytoplasmic inclusions, with loss of the normal nuclear expression. The mechanisms leading to TDP-43 redistribution and its role in disease pathophysiology remain unknown. We describe an *in vitro* neural tissue model that reproduces TDP-43 relocalization and inclusion formation. Two week-old coronal organotypic mouse brain slice cultures were treated with tunicamycin for 7 days. In cortical regions of treated slice cultures, cytoplasmic inclusions of TDP-43 immunoreactivity were observed, with loss of nuclear TDP-43 immunoreactivity. These inclusions were found in both astrocytes and neurons, and were of both skein-like and round morphologies. In contrast, TDP-43 cytoplasmic inclusions were not found in slices treated with staurosporine to induce apoptosis, or with trans-4-carboxy-L-proline (PDC) to induce chronic glutamate excitotoxicity. Furthermore, TDP-43 cytoplasmic inclusions did not co-localize with cleaved caspase-3, suggesting that TDP-43 mislocalization does not generally accompany caspase activation or apoptosis. The induction of TDP-43 cytoplasmic translocation in cerebrocortical slice cultures by tunicamycin provides a platform for further mechanistic investigations of pathological processing of TDP-43.

Keywords

Amyotrophic lateral sclerosis; frontotemporal lobar degeneration; tunicamycin; inclusions; caspase-3; apoptosis

Introduction

TAR-DNA binding protein (TDP-43) is a ubiquitous nuclear protein with roles in transcriptional repression and regulation of RNA splicing [1]. In neurodegenerative disorders including FTLD-U and ALS, TDP-43 is a major component of ubiquitin-positive inclusions in neurons and glia [2, 3]. Salient histopathological findings in affected cells in

© 2012 Elsevier B.V. All rights reserved.

Address correspondence to: Dr. James R. Brorson, Department of Neurology, MC2030, The University of Chicago, 5841 S. Maryland Ave., Chicago, IL 60637, Ph: 773-702-7215, Fax: 773-834-5435, jbrorson@neurology.bsd.uchicago.edu.

Publisher's Disclaimer: This is a PDF file of an unedited manuscript that has been accepted for publication. As a service to our customers we are providing this early version of the manuscript. The manuscript will undergo copyediting, typesetting, and review of the resulting proof before it is published in its final citable form. Please note that during the production process errors may be discovered which could affect the content, and all legal disclaimers that apply to the journal pertain.

NIH-PA Author Manuscript
NIH-PA Author Manuscript
NIH-PA Author Manuscript

NIH-PA Author Manuscript

NIH-PA Author Manuscript

NIH-PA Author Manuscript

ALS and most cases of FTLD-U include total or partial loss of nuclear TDP-43 with cytoplasmic redistribution and formation of insoluble aggregates [2–4]. FTLD-U is pathologically heterogeneous. In most cases, ubiquitin-positive cytoplasmic inclusions are found in cortical neurons of layer II of frontal and temporal cortex. Cytoplasmic inclusions are found with dense, Lewy-body-like shapes, and with skein-like morphologies. In other FTLD-U cases, neuronal intra-nuclear inclusions are also seen [5]. Glial cytoplasmic inclusions, positive for TDP-43 and ubiquitin, are reported in spinal cord tissues from sporadic ALS cases [3, 6]. In addition, non-ubiquitinated or lightly ubiquitinated TDP-43 inclusions have been described in subcortical white matter and in non-motor brain areas in cases with overlapping features of FTLD and motor neuron disease [6, 7].

The mechanisms leading to TDP-43 redistribution and aggregation in disease are unknown. In vivo, recent reports from transgenic mice have indicated that neuronal TDP-43 cytoplasmic aggregation and neurological dysfunction can result simply from brain overexpression of wild-type TDP-43 [8–10] as well as from expression of disease-associated mutant forms of TDP-43 [11]. Several attempts have also been made to reproduce TDP-43 redistribution and aggregate formation in vitro [12–14]. In a yeast model, over-expression of fluorescently tagged wild-type TDP-43 produced aggregate formation and growth arrest [13]. Over-expression of truncated forms of TDP-43 in SH-SY5Y cells also produced TDP-43 inclusions [14]. Given the known link of some forms of FTLD-U to progranulin gene mutations [15], other studies explored effects of progranulin suppression on TDP-43, producing conflicting evidence. Suppression of progranulin in HeLa cells induced caspase-dependent proteolytic cleavage of TDP-43 and redistribution to the cytoplasm, paralleling the effects of staurosporine treatment [12]. Other investigators did not observe a significant redistribution of TDP-43 upon reduction of progranulin expression in human cell lines and in zebra fish [16]. The mechanisms producing redistribution of natively expressed TDP-43 in differentiated neurons or glia remain incompletely understood.

The relation between TDP-43 proteinopathy and disease pathogenesis is not fully established. Loss of TDP-43 nuclear function may lead to transcriptional dysregulation and abnormal messenger RNA splicing, producing cellular toxicity. Indeed, transgenic mice with overexpression of disease-associated mutant forms of TDP-43, or of TDP-43 lacking the nuclear localization sequence, developed motor neuron degeneration without identifiable cytoplasmic aggregates, supporting a loss-of-function mechanism [11, 17]. On the other hand, cytoplasmic inclusion formation may be key to the loss of nuclear function of TDP-43, as in vitro induction of cytoplasmic inclusion formation through over-expression of either truncated TDP-43 protein, or of an aggregate-forming polyglutamine sequence, was sufficient to drive recruitment of native full-length TDP-43 into the inclusions, resulting in loss of normal nuclear TDP-43 localization and function [14, 18]. Alternatively, correlation of production of C-terminal fragments of TDP-43 with disease development and progression in transgenic mice has been interpreted as suggesting a toxic gain of function of misprocessed TDP-43 [10].

In this study, we describe TDP-43 redistribution and inclusion formation in an organotypic mouse brain slice culture model. Organotypic cultures offer several advantages for in vitro study of protein redistribution. As compared with dissociated cultures, organotypic slice cultures are hardy, with neurons surviving in vitro for weeks, allowing prolonged treatments. In addition, a preserved cytoarchitecture provides for normal intercellular contacts and allows for identification of specific brain regions and cell types. Finally, in comparison to in vivo studies, slice cultures offer the advantage of efficient testing of multiple treatments in parallel, with more precise control of drug concentrations and exposure duration.

NIH-PA Author Manuscript

NIH-PA Author Manuscript

NIH-PA Author Manuscript

Using this system, we examined whether cytoplasmic redistribution of TDP-43 might be induced by prolonged exposures to various cell stressors, applying staurosporine, the glutamate uptake inhibitor PDC, and tunicamycin, and thereby triggering apoptosis, excitotoxicity, and intracellular accumulation of secreted proteins, respectively. Our results indicate that while cytotoxic treatments do not, in general, cause TDP-43 relocalization, treatment with tunicamycin results in TDP-43 redistribution and inclusion formation, independently of caspase activation.

Materials and Methods

Organotypic Tissue Cultures and treatments

Cerebrocortical organotypic slice cultures from newborn pups of C57BL/6 mice were generated and maintained as previously described [19]. Slices (initial thickness 385 μm) were from frontal brain areas including motor cortex. Animal procedures followed protocols approved by the University of Chicago Animal Care and Use Committee. After two weeks in culture, slices were treated with 0.1 – 1 μg/ml tunicamycin (from 1 mg/ml stock in dimethylsulfoxide; Sigma T7765, lot numbers 087K4125 and 029K4008). Based on weighted averages of reported tunicamycin homologue compositions of these lots, average formula molecular weights of 861.2 g/mol and 856.2 g/mol were calculated, yielding an equivalent molar concentration of ~1.2 μM for the 1 μg/ml concentration of tunicamycin. Sister cultured slices were treated with 1 nM – 1 μM staurosporine (Cell Signaling Technology; Beverly, MA), 50 μM PDC (Tocris; Bristol, UK), or with vehicle alone (0.1% dimethylsulfoxide in culture medium). Treatments continued for 7 days, reapplied with the mid-week feeding.

Immunohistochemistry

After treatments, organotypic brain slices were fixed in 4% paraformaldehyde in phosphate-buffered saline (PBS), at 37°C, washed, permeablized in 0.1% Triton X-100 (Sigma) in PBS, and left in blocking buffer (1.5% donkey serum in Triton X-100/PBS) overnight at 4°C. Slices were then excised, attached to a fragment of the supporting membrane, and placed in primary antibody in blocking buffer, for overnight incubation at 4 °C. Primary antibodies employed include those directed to TDP-43 (affinity-purified rabbit polyclonal antibody to TARDBP, ProteinTech Group, Chicago. IL; at 1:1000 titer), MAP-2 (mouse monoclonal MAb3418, Chemicon, Temecula, CA; at 1:300), GFAP (mouse monoclonal clone Ab-6, Thermo Scientific, Fremont, CA; at 1:300), NeuN (mouse monoclonal MAb377, Chemicon; at 1:300), α-synuclein (mouse monoclonal anti-α-synuclein, Chemicon; at 1:1000), and ubiquitin (mouse monoclonal MAb1510 Chemicon; at 1:1000). After washing, slices were then incubated overnight at 4°C in secondary antibody (Cy2–conjugated donkey-anti-mouse IgG H+L and Cy5-conjugated donkey-anti -rabbit IgG H+L antibodies, at 1:250 dilutions; Jackson Immunoresearch, West Grove, PA). Double immunofluorescence detection of TDP-43 and cleaved caspase -3 was achieved with directly fluorescently labeled antibodies. The affinity-purified polyclonal TDP-43 antibody was tagged with Alexa Fluor 647 using a commercial kit (Invitrogen/Molecular Probes, Carlsbad, CA), and applied with an anti-cleaved-caspase-3 (Asp 175) antibody-Alexa Fluor 488 conjugate (Cell Signaling Technology). Slices were counterstained in Hoechst 33342 dye (10 μg/ml; Invitrogen) for 20 min, washed, and mounted on glass slides in Fluoro-G mounting solution (Southern Biotech, Birmingham, AL), with the membrane support facing the slide.

Protein fractionation and Western blotting

Cultured brain slices were washed in PBS, lifted from membrane supports, and transferred to microfuge tubes on ice. Samples were lysed in lysis buffer (20mM Tris-HCl, pH 7.4, 150

NIH-PA Author Manuscript

NIH-PA Author Manuscript

NIH-PA Author Manuscript

mM NaCl, 1 mM EDTA, 0.5% Triton X-100, 0.5% Na-deoxycholate) containing 1x protease inhibitors (Roche, Indianapolis, IN). The lysate was sonicated, and centrifuged at 4°C for 30 min at 100,000 × g in a Sorvall RC M120EX ultramicrocentrifuge and T-100 rotor, to generate the soluble (S) and pellet (P) fractions. Equal S and P fractions were subjected to Western blotting. Proteins were separated by 14% SDS-PAGE, and transferred to PVDF membranes. Membranes were blocked in 5% nonfat powdered milk, and probed with the affinity-purified antibody against full-length TDP-43 described above, at 1:500, and with goat-anti-rabbit IgG secondary antibody (1:5000; Santa Cruz Biotechnology, Santa Cruz, CA). Signal was detected on a Chemi Doc XRS imager (Bio-Rad, Hercules, CA), using SuperSignal West Pico chemiluminescent substrate (Pierce, Rockford, IL).

Microscopy

Images were obtained using an Olympus DSU spinning disc confocal microscope, using excitation and emission channels appropriate for each fluorophore. A defined protocol was followed to sample a consistent cortical region, corresponding to dorsolateral sensorimotor cortex. Under the 2x objective, a sampling transect was selected along a line angled at 25 degrees from the interhemispheric fissure of the brain slice. Then, with a 60x water-immersion objective, images were obtained along this transect at approximate distances of 200 μm from the gray-white matter junction and 200 μm from the pial surface. These sampling locations corresponded to the locations of cortical Layers V and II/III, as determined based on measurement of positions of non-phosphorylated neurofilament-positive pyramidal neurons in untreated cultures. For TDP-43 aggregate quantification, confocal images were obtained at these standard sampling locations, in stacks of 0.5 – 1.0 μm optical sections spanning depths ranging from 5 to 15 μm below the surface of the slice. For nuclear immunoreactivity analysis, sets of 3 single confocal optical sections, in contiguous high-power fields, were obtained in each cortical layer and in each hemisphere, at a depth of 10 μm, at constant settings for exposure times, camera gain, and thresholding. Some selected images were obtained with a laser confocal microscope with a 63x oil immersion objective to produce single optical sections with greater resolution.

Data Acquisition and Statistical Analysis

Images were processed and analyzed using the software program ImageJ, version 1.41b. Color images were compiled from individual channel Z-stacks using ImageJ, and assigning blue, green, and red pseudocolor values to the Hoechst, Cy2, and Cy5/TDP-43 channel images, respectively. Quantification of TDP-43 inclusions was performed by manual counting on Z stacks of color images, using the Image J Cell Counter macro and stereological methods. For quantification of nuclear TDP-43 intensity, a software macro was created to identify nuclear outlines in the Hoechst channel image. Outlines were then superimposed over the Cy5/TDP-43 channel and gray intensity values were obtained for the area within the outlines. Background intensity values were obtained from parallel organotypic slices incubated only in secondary antibody and Hoechst stain using the protocol outlined above. After background subtraction, average pixel intensity values were normalized by the mean value across conditions within the experimental replicate. Results were compared by one-way ANOVA on Ranks.

All experiments were repeated in independent replicate sets from multiple slice culture dates. Data are reported as mean ± standard error of the mean (SEM). Statistical testing utilized SigmaStat 2.0 (Systat Software Inc).

NIH-PA Author Manuscript

NIH-PA Author Manuscript

NIH-PA Author Manuscript

Results

Tunicamycin Induces TDP-43 Cytoplasmic Aggregation in Brain Slices

We examined the effects of three distinct cellular stressors on TDP-43 localization in organotypic slice cultures of mouse brain frontal cortex. Two week-old cultured slices were subjected to prolonged (7 day) exposures to either the protein kinase inhibitor staurosporine (1 nM), the glutamate transporter inhibitor trans-4-Carboxy-L-proline (PDC, 50 μM), or the protein N-glycosylation inhibitor tunicamycin (1 μg/ml; TDP-43 inclusions in cerebral slice cultures approximately 1.2 μM). These treatments induce, respectively, caspase activation, chronic glutamate-mediated excitotoxicity, and disruption of processing of secreted proteins. Low concentrations were chosen, aiming to produce cellular stress over prolonged treatments, without widespread apoptosis or cell death. After treatment for 7 days, slices were fixed, immunostained for TDP-43, counterstained with Hoechst dye, and visualized using confocal microscopy. Images were obtained from predefined dorsolateral cortical areas, encompassing layers II/III and V in sensorimotor cortical areas known to be affected in pathologies associated with TDP-43 relocalization.

In untreated controls, or in 0.1% DMSO vehicle-treated slices, TDP-43 localized to nuclei, evidenced by co-localization with Hoechst dye fluorescence (Figure 1A). TDP-43 immunoreactivity was near background levels in non-nuclear areas in these slices. In contrast, tunicamycin-treated slice cultures showed brightly stained inclusions of TDP-43 immunoreactivity outside the nuclear profiles. In addition, the nuclear TDP-43 immunoreactivity was faint or absent in some nuclei in tunicamycin-treated slices. The extranuclear TDP-43 inclusions generally lay immediately adjacent to nuclei, consistent with a cytoplasmic location. In staurosporine- and PDC-treated slice cultures, no such extranuclear inclusions of TDP-43 were observed (Figure 1A). PDC-treated slices included some swollen nuclei consistent with excitotoxicity, but nuclei generally retained TDP-43 immunoreactivity. However, occasional pyknotic nuclei lacked TDP-43 immunoreactivity. Staurosporine produced little or no change in TDP-43 distribution relative to controls. In some staurosporine-treated slice cultures, an increase in numbers of pyknotic or fragmented nuclei was observed, but without any associated TDP-43 inclusions.

To quantify the effects of tunicamycin on TDP-43 inclusion formation, confocal images were obtained from dorsolateral cortex in an unbiased fashion, followed by counting of cells with or without cytoplasmic TDP-43 inclusions. These studies revealed that, on average, 8.9 ± 2.1% (mean ± S.E.M.) of cells sampled in tunicamycin-treated slices contained cytoplasmic inclusions, compared to 0% in staurosporine-treated, PDC-treated, or vehicle-treated slices (Figure 1B; $n = 7$; $p < 0.001$ by one way ANOVA on Ranks).

As loss of nuclear function of TDP-43 may contribute to the pathophysiology of neurodegenerative diseases characterized by its redistribution, we also quantified the effect of chronic tunicamycin treatment on nuclear TDP-43 content. Nuclear immunoreactivity of TDP-43 was measured using average background-subtracted pixel intensity values within nuclear outlines. Intensity was measured from all nuclei within the plane of the optical section, without selection for cells showing cytoplasmic TDP-43 inclusions. Tunicamycin treatment decreased the relative intensity of nuclear immunoreactivity for TDP-43 by more than one third, compared to controls (Figure 1C; $n = 7$; $p < 0.001$ by one-way ANOVA on Ranks). In contrast, staurosporine-treated or PDC-treated cultures showed no significant decrease in nuclear immunoreactivity compared to controls. A trend towards a decrease in PDC-treated cells possibly related to nuclear swelling.

In separate experiments, we also examined the time course of appearance of TDP-43 inclusions in slices treated with tunicamycin (Figure 1D). Few inclusions were present after

NIH-PA Author Manuscript

NIH-PA Author Manuscript

NIH-PA Author Manuscript

only 1 or 3 days of treatment, with greater numbers of inclusions appearing after 7 days, significantly more than in parallel controls, in which none were found (n = 4; p = 0.03 by one-way ANOVA on Ranks).

Characterization of TDP-43 inclusions

In FTLD-U, the cytoplasmic redistribution of TDP-43 has been described primarily in neurons, while in ALS, it has been seen in both neurons and glia of the spinal cord [3, 20]. To confirm the intracellular location of the tunicamycin–induced TDP-43 inclusions, and to determine the affected cell type, slices were doubly immunostained for TDP-43 and for either an astrocytic marker, glial fibrillary acidic protein (GFAP), or a neuronal marker, microtubule-associated protein-2 (MAP-2). Cytoplasmic TDP-43 inclusions in tunicamycin-treated cultures were found in both glia and neurons, within the cytoplasmic volumes defined by the GFAP or MAP-2 distributions (Figure 2). In blinded counts from 3 independent replicates, 37% GFAP-labeled astrocytes and 7% of MAP-2– immunoreactive neurons exhibited cytoplasmic TDP-43 inclusions after tunicamycin treatment, whereas none were found in GFAP- or MAP-2-stained cells in control slices (Table). Inclusions were found in both cortical layers II/III and layer V. In shape, the inclusions varied from compact, rounded densities reminiscent of Lewy bodies (arrowhead, Figure 2B), to looser, reticulated or skein-like clusters (arrows). In other examples, cells with a diffuse cytoplasmic distribution of intense TDP-43 immunoreactivity could be seen (not shown). No neuronal intra-nuclear inclusions were noted.

In diseased brain and spinal cord preparations, cytoplasmic TDP-43 inclusions are generally ubiquitinated [21]. In control organotypic slice cultures, ubiquitin immunoreactivity was found in a somatodendritic distribution in neuron-like cells (Figure 3A), with high background staining. In slices treated with tunicamycin, a similar ubiquitin distribution was found in cells retaining the normal nuclear localization of TDP-43 immunoreactivity. Inclusions with intense ubiquitin immunoreactivity were not found. The tunicamycin-induced cytoplasmic TDP-43 inclusions displayed only weak co-staining for ubiquitin (Figure 3B).

We also evaluated whether protein redistribution and inclusion formation was a general effect of tunicamycin treatment. In contrast to the cytoplasmic mislocalization of TDP-43 immunoreactivity in tunicamycin-treated slices, there was no evidence of altered distribution of the nucleo-somatic neuron-specific protein NeuN, or of the somato-dendritic localization of α-synuclein (not shown).

No evidence for insoluble TDP-43 fragments in tunicamycin-treated slices

In FTLD-U–affected brain, and in some cellular models of TDP-43 pathology, evidence for accumulation of 24–26 kD fragments of TDP-43 has been described [2]. We therefore examined the distribution of soluble and insoluble fractions of whole cell protein preparations from organotypic slices treated with tunicamycin for 7 days, by Western blotting with the polyclonal antibody to TDP-43. Other samples were treated overnight with staurosporine (0.3 μM). No consistent shift in the distribution of TDP-43 from the soluble fraction to the pellet with tunicamycin treatment was found. In all samples, only a single band with a migration rate of ~43 kD, was detected, without detection of smaller fragments of TDP-43 (not shown).

Dissociation of TDP-43 aggregation and apoptosis

As described above, there was no evidence of TDP-43 redistribution in slices treated for 7 days with staurosporine, using a low concentration (1 nM) chosen to avoid widespread cell death over the chronic treatment period. However, the low concentration of staurosporine

NIH-PA Author Manuscript

NIH-PA Author Manuscript

NIH-PA Author Manuscript

applied may have been insufficient to induce significant apoptosis, or the 7 day interval before observation may have missed early effects of staurosporine on TDP-43 distribution. Higher concentrations of staurosporine have been reported to produce TDP-43 cytoplasmic aggregation in non-neuronal cells after brief exposures [12]. To test the effects of higher staurosporine concentrations on TDP-43 localization, we treated cultured slices with 0.3 μM and 1.0 μM staurosporine for 24 hours. These short-term staurosporine treatments produced more qualitative evidence of apoptosis, with greater numbers of pyknotic nuclei and apoptosome-like fragmented nuclei (Figure 4). However, even at these higher staurosporine concentrations, with 24 hour treatments, dense TDP-43 extranuclear inclusions like those in tunicamycin-treated slices were not observed. Instead, with induction of apoptotic changes in nuclear morphology, cells generally lost any TDP-43 immunoreactivity in both nuclei and cytoplasm.

We also examined effects of 7 day exposures to staurosporine at concentrations of 0.1, 0.3, and 1 μM, using immunostaining for cleaved caspase-3 to positively identify cells with caspase activation (Figure 5). Staurosporine treatment at these concentrations induced the appearance of cells with diffuse cytoplasmic staining for cleaved caspase-3, associated with small pyknotic nuclei, again with loss of TDP-43 immunoreactivity (Figure 5B). Such apoptotic cells were seen to a lesser extent also in slices treated with tunicamycin for 7 days. However, in blinded examination of all the confocal images from these experiments, none of the numerous cleaved caspase-3 positive cells in staurosporine-treated slices were found to contain cytoplasmic TDP-43 inclusions. Furthermore, blinded counting again showed that staurosporine, while activating caspase-3 at all concentrations applied, failed to trigger significant numbers of cytoplasmic TDP-43 inclusions (Figure 5D, E). In slices treated with tunicamycin, the TDP-43 inclusions that occurred were virtually all in cells lacking activation of caspase-3 (75 of 77 cells). Thus, both by cellular location and by treatment condition, caspase activation was dissociated from TDP-43 cytoplasmic inclusion formation, providing evidence that induction of apoptosis and caspase activation is neither necessary nor sufficient to induce TDP-43 cytoplasmic relocalization in neural tissues.

Discussion

The identification of TDP-43 as a major component of cytoplasmic inclusions in FTLD-U and ALS provided an important advance in the understanding of the pathophysiology of these conditions. In vitro models of molecular events associated with degenerative diseases can assist mechanistic investigations and assessments of candidate treatments. While previous studies have established that TDP-43 redistribution can be induced by over-expression in immortalized cell lines [12–14], an in vitro model producing redistribution of natively expressed TDP-43 in cells of primary neural tissues may provide greater relevance to disease pathophysiology. Here we report that cytoplasmic relocalization of endogenous TDP-43 in differentiated neurons and glia of cultured brain slices is produced by chronic treatment with tunicamycin. TDP-43 inclusions were cytoplasmic, variable in morphology, and associated with depletion of nuclear TDP-43. Thus this model recapitulates several of the important features of cortical changes in FTLD-U brains, and has the potential to facilitate study of CNS-specific mechanisms of disease pathogenesis.

While week-long tunicamycin exposure, a stressful and potentially toxic treatment, led to cytoplasmic TDP-43 inclusion formation, it is notable that neither a common experimental stimulus of apoptotic pathways, staurosporine, nor one of chronic excitotoxic death, the glutamate transport inhibitor PDC, induced such TDP-43 redistribution. Our model thus establishes that TDP-43 relocalization is not a general effect of cellular stress, and does not invariably accompany apoptosis. Furthermore, the appearance of cytoplasmic inclusions of TDP-43 in this model was generally dissociated from markers of apoptosis such as nuclear

NIH-PA Author Manuscript

NIH-PA Author Manuscript

NIH-PA Author Manuscript

condensation or caspase-3 activation, suggesting that apoptosis is neither necessary nor sufficient to produce TDP-43 relocalization in cultured brain slices.

These findings in organotypic brain slice cultures differ from those reported originally in HeLa cells, in which staurosporine treatment induced TDP-43 cytoplasmic inclusions via caspase-induced cleavage of TDP-43 [12]. Others have confirmed that caspase activation can induce TDP-43 cleavage in mouse embryonic fibroblasts or NSC-34 cells [22, 23, 24]. However, cytoplasmic aggregation of full-length TDP-43 is reported to occur even when caspase inhibitors were applied to prevent TDP-43 cleavage [23], and caspase-induced TDP-43 cleavage reportedly protected against TDP-43-induced cell death, rather than promoting it [24]. It may be that staurosporine-induced, caspase-dependent TDP-43 cleavage and aggregation is a cell-specific phenomenon, not prominently occurring in neural tissues. In any case, the evidence suggests that caspasemediated cleavage of TDP-43 is not an essential step in production of TDP-43 – associated pathology in neurons.

The mechanism by which tunicamycin induces TDP-43 redistribution and inclusion formation in this model is unknown. One possibility is that tunicamycin, by interference with protein glycosylation, has a general detrimental effect on global protein processing by cells. However, we found no evidence for cytoplasmic re-localization of another nuclear protein, Neu-N, nor for aggregate formation of α-synuclein, another cytoplasmic protein prone to aggregation, nor for qualitative changes in distributions of GFAP, MAP-2, or non-phosphorylated neurofilament proteins. Thus the evidence weighs against a non-specific effect on general cellular protein processing affecting the distribution of numerous proteins. Other recent in vitro work has established that pharmacological disruption of the ubiquitin-proteasomal system in cultured cells with MG132 is sufficient to induce increased cytoplasmic redistribution on TDP-43 in fibroblasts or cortical neurons [23], suggesting that disruption of cellular protein processing and disposal may lead to TDP-43 redistribution. Thapsigargin, an agent inducing endoplasmic reticulum (ER) stress, was also shown to enhance TDP-43 cleavage in undifferentiated NSC-34 cells, without demonstration of its effects on TDP-43 distribution [24]. It may be that these agents, as well as tunicamycin, are all acting via stimulation of the ER stress response to indirectly disrupt TDP-43 production, proper conformation, and nuclear localization. This hypothesis merits further investigation.

Alternatively, tunicamycin may affect TDP-43 distribution through a mechanism related to disruption of secretion of progranulin, a molecule linked in familial frontotemporal dementia cases to TDP-43 proteinopathy [3, 4]. Progranulin is a heavily glycosylated protein, and suppression of progranulin has been reported in several in vitro studies to produce misprocessing of TDP-43 [12, 23, 25]. Kleinberger et al. [23] reported that progranulin knockout alone was sufficient to produce increased phosphorylation of TDP-43 in cortical neurons, while only with the additional stress of proteasomal inhibition was there TDP-43 fragmentation and accumulation of insoluble aggregates. Guo et al. [25] reported that progranulin knockdown by siRNA in primary cortical neurons produced cytoplasmic relocalization of TDP-43 and increased neuronal vulnerability to toxins in a fashion that could be ameliorated by overexpression of progranulin. Thus it is possible that tunicamycin produces TDP-43 misprocessing by the combined suppression of progranulin secretion and stimulation of ER stress.

In our experiments, TDP-43 cytoplasmic inclusions were observed in both MAP-2 -positive neurons and GFAP-positive glial cells. In FTLD-U brains, cytoplasmic inclusions were initially described in neurons [2]. The neuronal cytoplasmic inclusions have been found most prominently in layer II rather than layer V of frontal cortex [5], and in spinal motor neurons of sporadic and some types of familial ALS [4]. In addition to neuronal inclusions, subsequent studies have recognized frequent TDP-43 inclusions in oligodendrocytes of

NIH-PA Author Manuscript

NIH-PA Author Manuscript

NIH-PA Author Manuscript

cortical white matter in most FTLD-U cases [26], and in both glia and neurons of non-motor nuclei and cortex in sporadic ALS cases [6]. The latter were especially noted in those ALS cases associated with dementia, and these TDP-43 inclusions, like those in the present model, were only weakly immunoreactive for ubiquitin [6]. TDP-43 inclusions of 'linear wisp' or 'fine skein' morphology, features taken to suggest an early stage of inclusion formation, were found to stain weakly for ubiquitin [27]. In the present model, it may be that the relatively short duration of tunicamycin exposure, as compared to the decades of pathology affecting FTLD brains, also produces primarily early stage TDP-43 inclusions, lacking strong ubiquitination.

A limitation of the present model is that the accumulation of insoluble shorter length fragments of TDP-43, as described in chronic brain material from FTLD-U patients [2, 3], was not confirmed. It is notable that studies of material in the yeast model of TDP-43 proteinopathy also failed to detect TDP-43 fragmentation [13]. In the present model only a fraction of cells exhibit TDP-43 pathology, and the total recovered protein amounts are small. The sensitivity of immunoblotting may be insufficient to detect minute amounts of TDP-43 fragments present in the slices. Alternatively, it may also be that accumulation of such insoluble fragments is a process with slow kinetics, occurring as the disease progresses over many years, but not in shorter-term models that still produce TDP-43 relocalization.

The minute amounts of tissue available from organotypic slice cultures limits the applicability of this model for protein chemistry studies such as preparations of subcellular fractions comparing nuclear and cytoplasmic TDP-43 components; for such studies, immortalized cell lines may be more suitable. The organotypic slice model has other practical limitations as compared to in vivo disease models. Slice preparation severs the connectivity of tracts between brain areas, potentially altering cellular physiology. Effects of vascular, endocrine, or immune systems influences that may influence cellular pathology are not present in the in vitro environment. Behavioral effects cannot be studied. However, in all respects pertaining to the immediate tissue environment of affected cells, the organotypic slice model better approximates the in vivo setting than does a dissociated culture model.

The present findings establish an *in vitro* brain-slice model for the study of TDP-43 relocalization, with the formation of cytoplasmic inclusions of native TDP-43 in neurons, independent of caspase activation and apoptosis. The mechanism by which tunicamycin induces TDP-43 cytoplasmic redistribution is the subject of ongoing investigations. This model, with its preserved cortical cytoarchitecture and robust reproduction of TDP-43 redistribution, provides a tractable platform for investigating such questions of the cellular pathophysiology of TDP-43 proteinopathy, changes that potentially underlie FTLD-U and ALS.

Acknowledgments

We wish to thank Vytautas Bindokas at the University of Chicago imaging lab for his support with image acquisition and processing, and Simren Dulai for assistance with slice cultures and staining.

This work was supported in part by funding from the Brain Research Foundation, the Pioneer Fund, and R01NS046037 (JM).

References

1. Wang I-F, Reddy NM, Shen C-KJ. Higher order arrangement of the eukaryotic nuclear bodies. Proc Natl Acad Sci. 2002; 99:13583–13588. [PubMed: 12361981]

NIH-PA Author Manuscript NIH-PA Author Manuscript NIH-PA Author Manuscript

2. Neumann M, Sampathu DM, Kwong LK, Truax AC, Micsenyi MC, Chou TT, et al. Ubiquitinated TDP-43 in frontotemporal lobar degeneration and amyotrophic lateral sclerosis. Science. 2006; 314:130–133. [PubMed: 17023659]
3. Arai T, Hasegawa M, Akiyama H, Ikeda K, Nonaka T, Mori H, et al. TDP-43 is a component of ubiquitin-positive tau-negative inclusions in frontotemporal lobar degeneration and amyotrophic lateral sclerosis. Biochem Biophys Res Commun. 2006; 351:602–611. [PubMed: 17084815]
4. Kwong LK, Neumann M, Sampathu DM, Lee VM-Y, Trojanowski JQ. TDP-43 proteinopathy: The neuropathology underlying major forms of sporadic and familial frontotemporal lobar degeneration and motor neuron disease. Acta Neuropathol. 2007; 114:63–70. [PubMed: 17492294]
5. Mackenzie IRA, Baborie A, Pickering-Brown S, Plessis DD, Jaros E, Perry RH, et al. Heterogeneity of ubiquitin pathology in frontotemporal lobar degeneration: Classification and relation to clinical phenotype. Acta Neuropathol. 2006; 112:539–549. [PubMed: 17021754]
6. Nishihira Y, Tan C-F, Onodera O, Toyoshima Y, Yamada M, Morita T, et al. Sporadic amyotrophic lateral sclerosis: Two pathological patterns shown by analysis of distribution of TDP-43-immunoreactive neuronal and glial cytoplasmic inclusions. Acta Neuropathol. 2008; 116:169–182. [PubMed: 18481073]
7. Hiji M, Takahashi T, Fukuba H, Yamashita H, Kohriyama T, Matsumoto M. White matter lesions in the brain with frontotemporal lobar degeneration with motor neuron disease: TDP-43-immunopositive inclusions co-localize with p62, but not ubiquitin. Acta Neuropathol. 2008; 116:183–191. [PubMed: 18584184]
8. Tsai K-J, Yang C-H, Fang Y-H, Cho K-H, Chien W-L, Wang W-T, et al. Elevated expression of TDP-43 in the forebrain of mice is sufficient to cause neurological and pathological phenotypes mimicking FTLD-U. J Exp Med. 2010; 207:1661–1673. [PubMed: 20660618]
9. Xu YF, Gendron TF, Zhang YJ, Lin WL, D'Alton S, Sheng H, et al. Wild-type human TDP-43 expression causes TDP-43 phosphorylation, mitochondrial aggregation, motor deficits, and early mortality in transgenic mice. J Neurosci. 2010; 30:10851–10859. [PubMed: 20702714]
10. Wils H, Kleinberger G, Janssens J, Pereson S, Joris G, Cuijt I, et al. TDP-43 transgenic mice develop spastic paralysis and neuronal inclusions characteristic of ALS and frontotemporal lobar degeneration. PNAS. 2010; 107:3858–3863. [PubMed: 20133711]
11. Wegorzewska I, Bell S, Cairns NJ, Miller TM, Baloh RH. TDP-43 mutant transgenic mice develop features of ALS and frontotemporal degeneration. PNAS. 2009; 106:18809–18814. [PubMed: 19833869]
12. Zhang Y-J, Xu Y-f, Dickey CA, Buratti E, Baralle F, Bailey R, et al. Progranulin mediates caspase-dependent cleavage of TAR DNA binding protein-43. J Neurosci. 2007; 27:10530–10534. [PubMed: 17898224]
13. Johnson BS, McCaffery JM, Lindquist S, Gitler AD. A yeast TDP-43 proteinopathy model: Exploring the molecular determinants of TDP-43 aggregation and cellular toxicity. Proc Natl Acad Sci (USA). 2008; 105:6439–6444. [PubMed: 18434538]
14. Nonaka T, Kametani F, Arai T, Akiyama H, Hasegawa M. Truncation and pathogenic mutations facilitate the formation of intracellular aggregates of TDP-43. Hum Molec Gen. 2009; 18:3353–3364. [PubMed: 19515851]
15. Eriksen JL, Mackenzie IRA. Progranulin: Normal function and role in neurodegeneration. J Neurochem. 2008; 104:287–297. [PubMed: 17953663]
16. Shankaran SS, Capell A, Hruscha AT, Fellerer K, Neumann M, Schmid B, et al. Missense mutations in the progranulin gene linked to frontotemporal lobar degeneration with ubiquitin-immunoreactive inclusions reduce progranulin production and secretion. J Biol Chem. 2008; 283:1744–1753. [PubMed: 17984093]
17. Igaz LM, Kwong LK, Lee EB, Chen-Plotkin A, Swanson E, Unger T, et al. Dysregulation of the ALS-associated gene TDP-43 leads to neuronal death and degeneration in mice. J Clin Investigation. 2011; 121:726–738.
18. Fuentealba RA, Udan M, Bell S, Wegorzewska I, Shao J, Diamond MI, et al. Interaction with polyglutamine aggregates reveals a Q/N-rich domain in TDP-43. The J Biol Chem. 2010; 285:26304–26314.

NIH-PA Author Manuscript

NIH-PA Author Manuscript

NIH-PA Author Manuscript

19. Back A, Tupper KY, Bai T, Chiranand P, Goldenberg FD, Frank JI, et al. Ammonia-induced brain swelling and neurotoxicity in an organotypic slice model. Neurological Research. 2011; 33:1100–1108. [PubMed: 22196764]
20. Seelaar H, Schelhaas J, Azmani A, Kusters B, Rosso S, Majoor-Krakauer D, et al. TDP-43 pathology in familial frontotemporal dementia and motor neuron disease without progranulin mutations. Brain. 2007; 130:1375–1385. [PubMed: 17360763]
21. Leigh PN, Whitwell H, Garofalo O, Buller J, Swash M, Martin JE, et al. Ubiquitin-immunoreactive intraneuronal inclusions in amyotrophic lateral sclerosis. Morphology, distribution, and specificity. Brain. 1991; 114:775–788. [PubMed: 1646064]
22. Nishimoto Y, Ito D, Yagi T, Nihei Y, Tsunoda Y, Suzuki N. Characterization of alternative isoforms and inclusion body of the TAR DNA-binding protein-43. J Biol Chem. 2010; 285:608–619. [PubMed: 19887443]
23. Kleinberger G, Wils H, Ponsaerts P, Joris G, Timmermans J-P, Van Broeckhoven C, Kumar-Singh S. Increased caspase activation and decreased TDP-43 solubility in progranulin knockout cortical cultures. J Neurochem. 2010; 115:735–747. [PubMed: 20731760]
24. Suzuki H, Lee K, Matsuoka M. TDP-43-induced death is associated with altered regulation of Bim and Bcl-xL and attenuated by caspase-mediated TDP-43 cleavage. J Biol Chem. 2011; 286:13171–13183. [PubMed: 21339291]
25. Guo A, Tapia L, Bamji SX, Cynader MS, Jia W. Progranulin deficiency leades to enhanced cell vulnerability and TDP-43 translocation in primary neuronal cultures. Brain Research. 2010; 1366:1–8. [PubMed: 20888804]
26. Neumann M, Kwong LK, Truax AC, Vanmassenhove B, Kretzschmar HA, Deerlin VMV, et al. TDP-43-positive white matter pathology in frontotemporal lobar degeneration with ubiquitin-positive inclusions. J Neuropathol Exp Neurol. 2007; 66:177–183. [PubMed: 17356379]
27. Mori F, Tanji K, Zhang H-X, Nishihira Y, Tan C-F, Takahashi H, et al. Maturation process of TDP-43-positive neuronal cytoplasmic inclusions in amyotrophic lateral sclerosis with and without dementia. Acta Neuropathol. 2008; 116:193–203. [PubMed: 18560845]

NIH-PA Author Manuscript

NIH-PA Author Manuscript

NIH-PA Author Manuscript

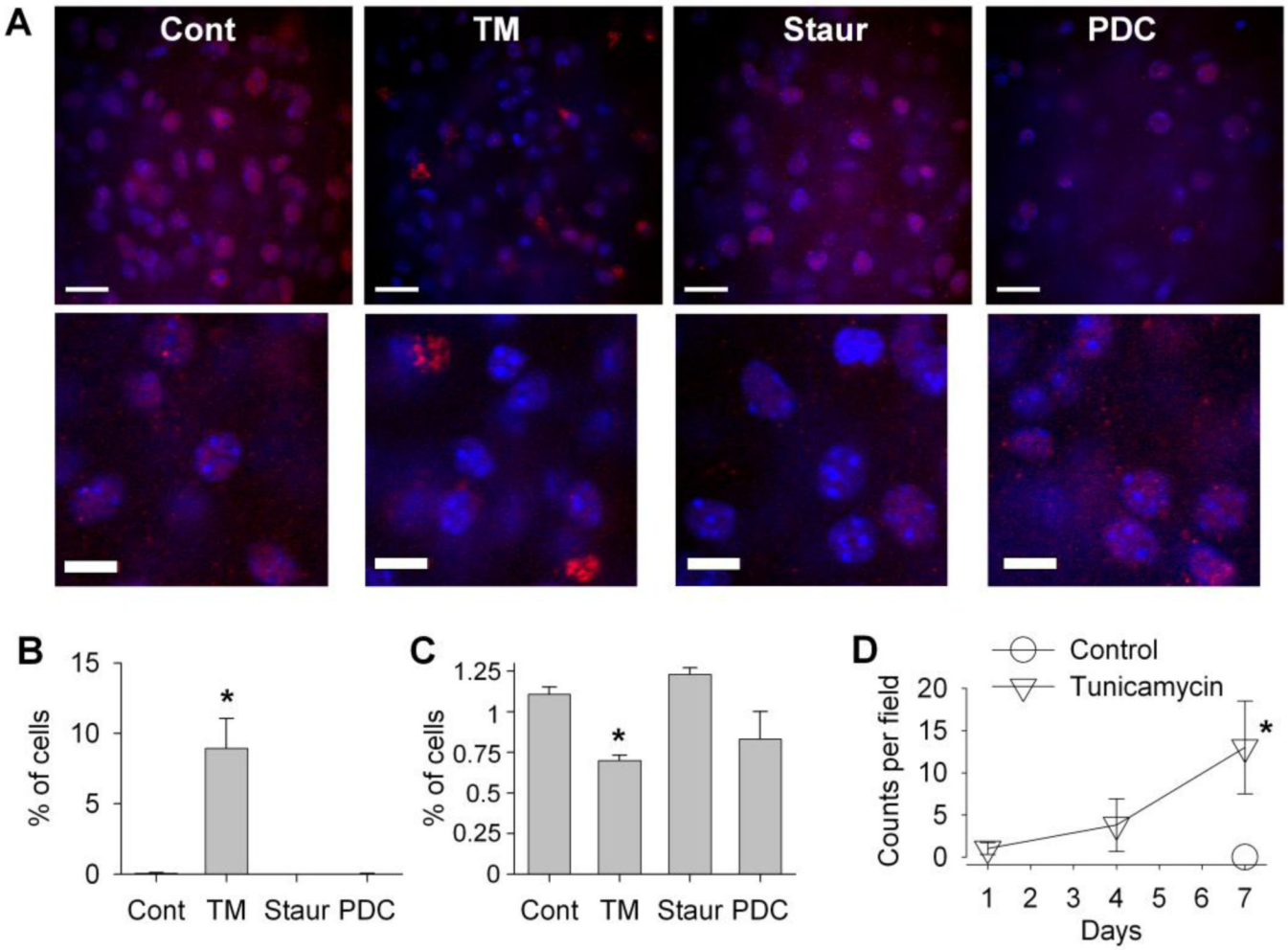

Figure 1. Tunicamycin induces formation of TDP-43 inclusions in cultured brain slices

A) Representative confocal optical sections from 3 week old cortical organotypic cultured slices, after 7 day treatments with tunicamycin (TM, 1 μg/ml), staurosporine (staur, 1 nM), PDC (50 μM), or control conditions (upper panels, full 60x field views, scale bar = 20 μm; lower panels, magnified views, scale bar = 10 μm). In control, staurosporine-treated, and PDC-treated slices, TDP-43 immunoreactivity (red) was restricted to a nuclear distribution, co-localizing with nuclear staining by Hoechst dye (blue). In contrast, in tunicamycin-treated slices, extranuclear inclusions of intense TDP-43 immunoreactivity were found adjacent to some nuclei. B) Percentages of cells containing extranuclear TDP-43 inclusions in each condition (mean ± SEM, n = 7; *p<0.001 by one-way ANOVA on ranks). C) Mean normalized background-subtracted intensity of nuclear immunoreactivity for TDP-43. Tunicamycin-treated cultures showed an overall 37% decrease in TDP-43 nuclear immunoreactivity compared to controls (mean ± SEM, n = 7; *p<0.001 by one-way ANOVA on ranks). D) Time course of appearance of cytoplasmic TDP-43 inclusions. Inclusions appeared in increasing numbers over 7 days of tunicamycin treatment (n = 4; *p = 0.03 by one-way ANOVA on ranks).

NIH-PA Author Manuscript

NIH-PA Author Manuscript

NIH-PA Author Manuscript

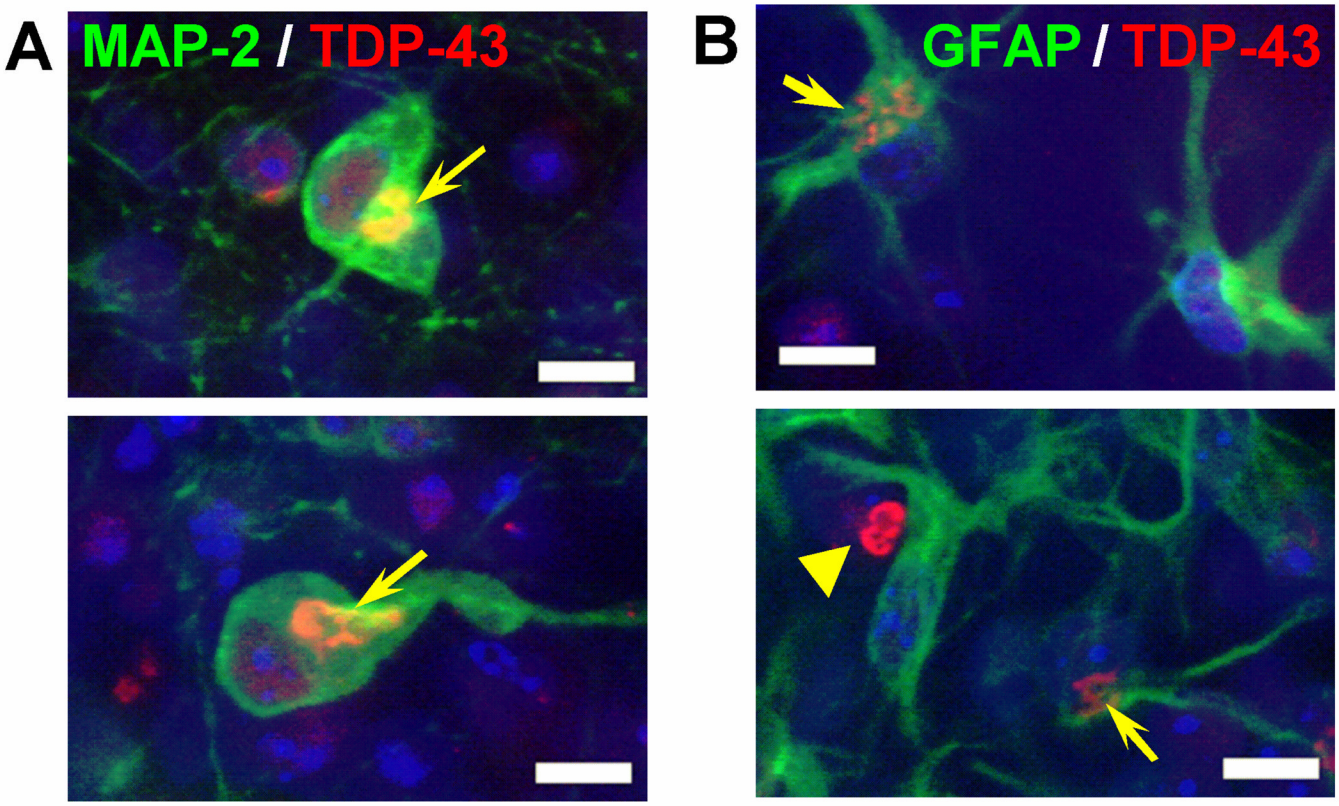

Figure 2. TDP-43 Inclusions found in MAP-2 Immunoreactive Neurons and Glial Cells

A) Selected confocal images of TM-treated organotypic slices, double immunostained for MAP-2 (green) and TDP-43 (red), and counterstained for nuclei (blue). Dense round or oblong inclusions of TDP-43 (arrows) were found within the cytoplasm of a minority of MAP-2 –positive neurons in TM-treated slices, but not in control slices. B) Double immunostaining for GFAP (green) and TDP-43 (red) similarly demonstrated cytoplasmic TDP-43 inclusions in GFAP-immunoreactive glial cells (arrows), generally with a reticulated or skein-like morphology. In addition, some inclusions showed a dense round morphology (arrowhead). No intranuclear inclusions were noted. (Scale bars = 10 μm).

NIH-PA Author Manuscript

NIH-PA Author Manuscript

NIH-PA Author Manuscript

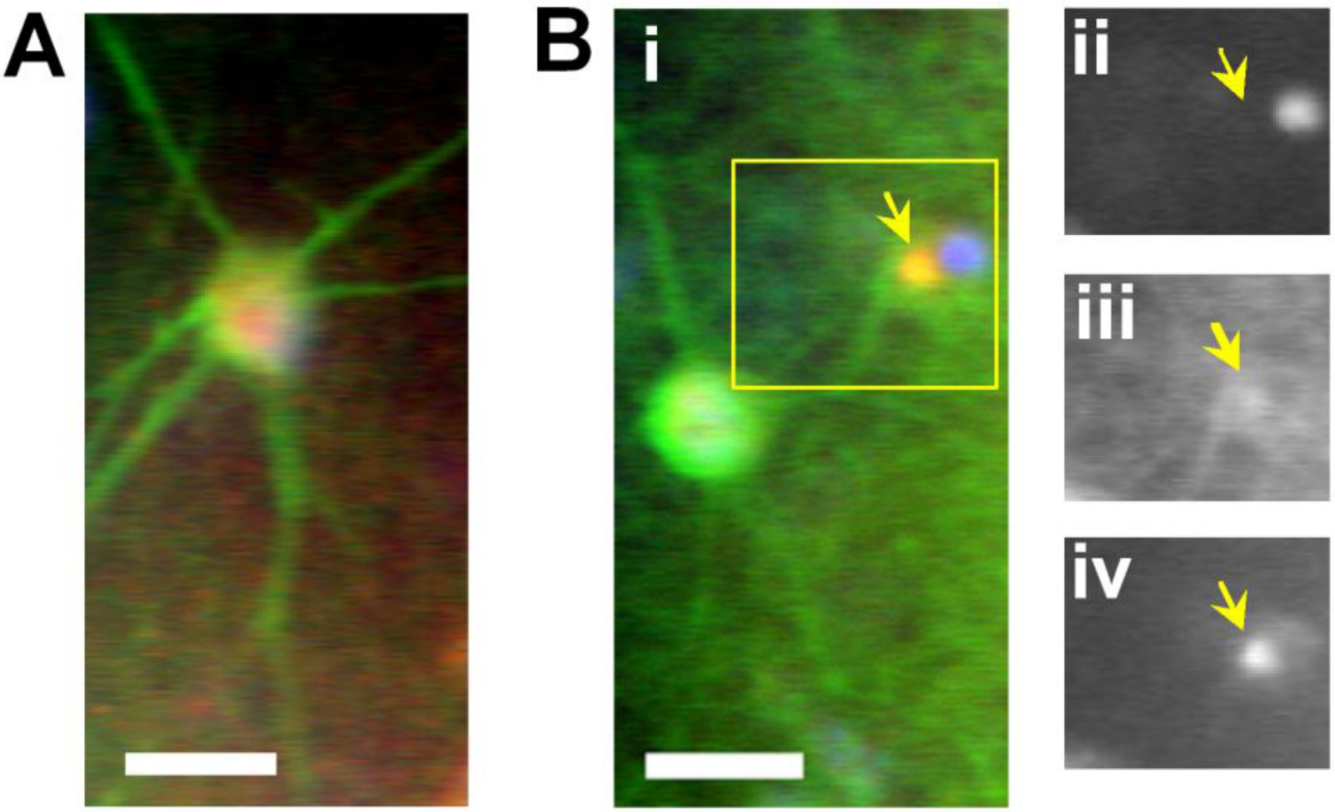

Figure 3. Double immunostaining for TDP-43 and ubiquitin

Representative confocal optical sections of double immunostaining for ubiquitin (green) and TDP-43 (red), with Hoechst staining of nuclei (blue). In control slices (A), ubiquitin immunoreactivity filled the somatic and dendritic profiles of neuron-like cells. In tunicamycin-treated slices (B), extranuclear TDP-43 inclusions, adjacent to the Hoechst-stained nucleus (panel ii) were not intensely stained for ubiquitin (panel iii), though light immunoreactivity for ubiquitin co-localized with inclusions of TDP-43 as well as distributing throughout the surrounding cytoplasm (panel iv). Arrows indicate the location of the TDP-43 inclusion in each panel (scale bar, 20 μm).

NIH-PA Author Manuscript

NIH-PA Author Manuscript

NIH-PA Author Manuscript

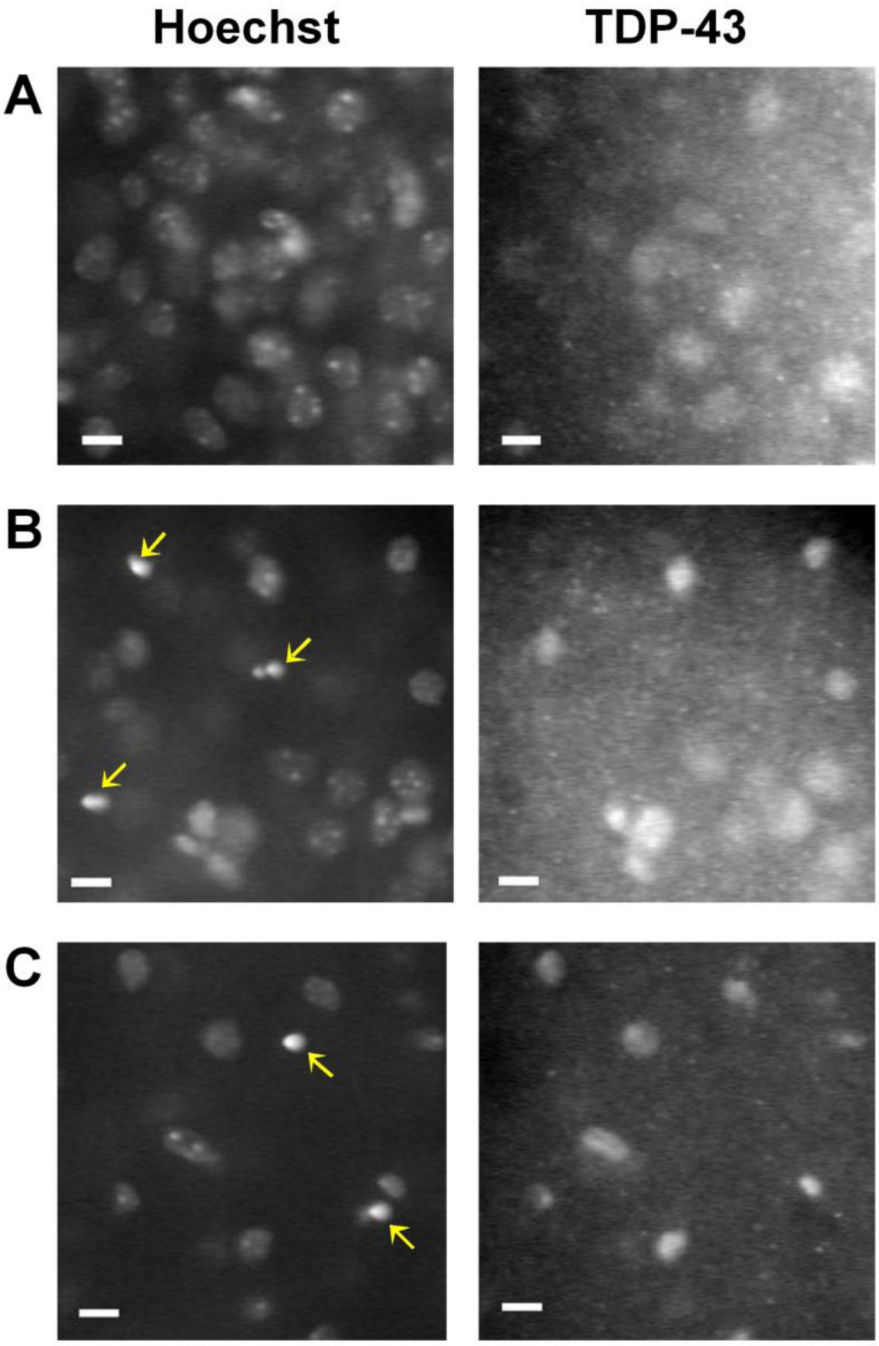

Figure 4. Lack of extranuclear TDP-43 inclusions in staurosporine-treated slice cultures

Representative optical sections from confocal images of organotypic slices immunostained for TDP-43 after 24 hour treatments with control conditions (A) or with 0.3 μM (B) or 1.0 μM (C) staurosporine. Left-hand column, Hoechst nuclear staining; right-hand column, TDP-43 immunoreactivity. Staurosporine treatment induced increasing frequency of apoptotic morphology, with pyknotic or fragmented nuclei (arrows), but extranuclear TDP-43 immunoreactive inclusions were not found.

NIH-PA Author Manuscript

NIH-PA Author Manuscript

NIH-PA Author Manuscript

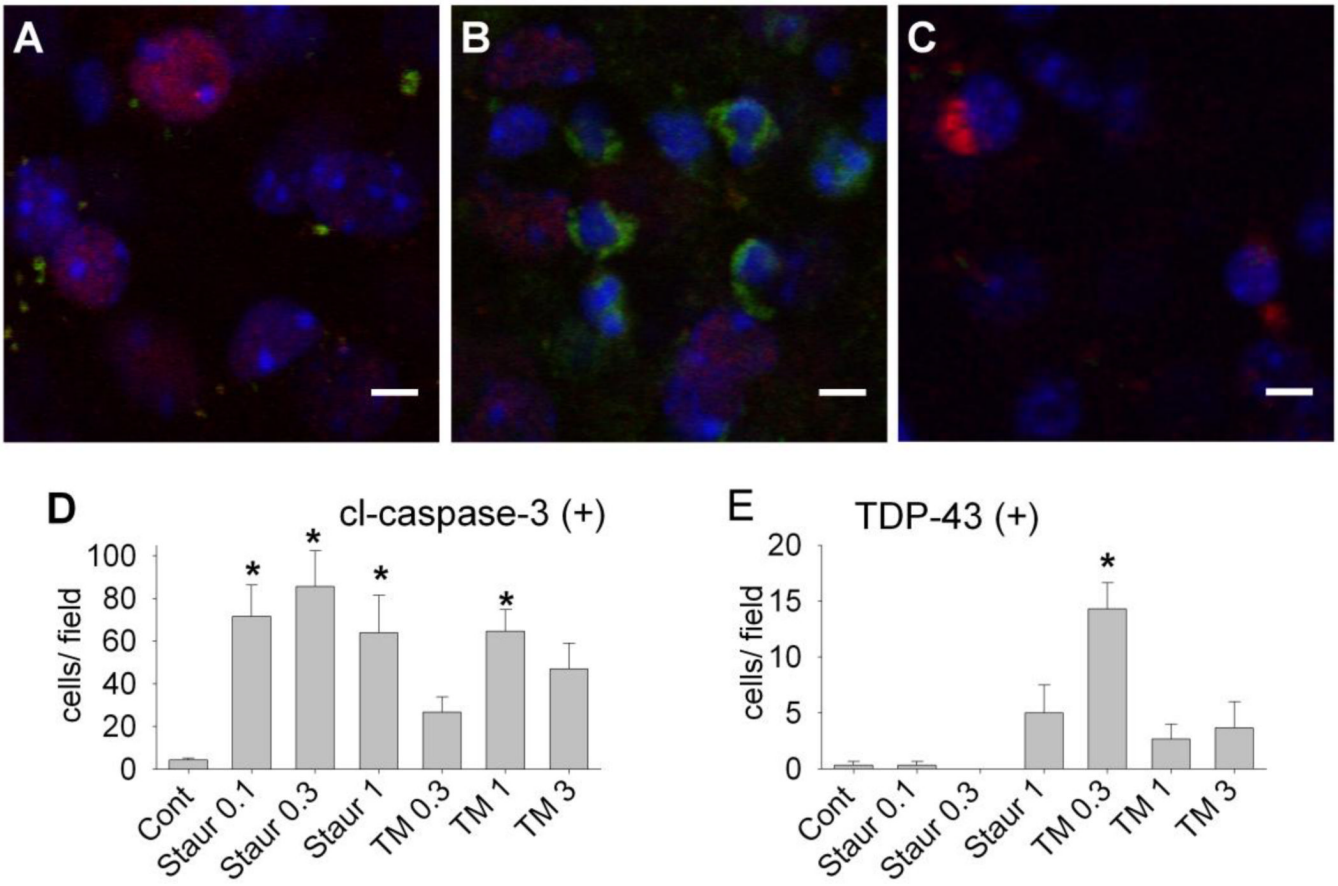

Figure 5. Dissociation of cleaved caspase-3 activation and TDP-43 aggregate formation

Laser scanning confocal images of organotypic slices immunostained for TDP-43 (red) and cleaved caspase-3 (green), with nuclear counterstaining (blue). Slices were treated for 7 days in control conditions, treated with vehicle 0.1% DMSO (A), with 0.3 μM staurosporine (B), or with 1 μg/ml tunicamycin (C) (scale bars, 5 μm). Cellular activation of caspase-3 was associated with nuclear pyknosis and loss of TDP-543 immunoreactivity, but not with cytoplasmic aggregation of TDP-43. D) Blinded counts of cells within confocal images stacks with cytoplasmic cleaved-caspase -3 staining showed significant caspase activation at all concentrations of staurosporine (0.1, 0.3, and 1 μM) but lesser activation by tunicamycin (0.3, 1, and 3 μg/ml) (n = 3; mean ± SEM, *p<0.05, one-way ANOVA). E) Counts of cells per field with cytoplasmic TDP-43 inclusions showed significant generation of TDP-43 redistribution only by tunicamycin 0.3 μg/ml, and not by any concentration of staurosporine (n = 3, mean ± SEM; * p < 0.05, one-way ANOVA).

NIH-PA Author Manuscript

NIH-PA Author Manuscript

NIH-PA Author Manuscript

Table

TDP-43 inclusions found in MAP-2- or GFAP-immunoreactive cells in control or tunicamycin-treated (TM, 1 μg/ml for 7 days) slices.

	Control	**TM-treated**
MAP-2 (+) cells	0 of 85 (0%)	8 of 122 * (7%)
GFAP (+) cells	0 of 40 (0%)	25 of 68 * (37%)

* $p < 0.05$ compared to control proportion, Fisher's exact test.